Friction Stir Welding and Processing V
Edited by: Rajiv S. Mishra, Murray W. Mahoney, and Thomas J. Lienert
TMS (The Minerals, Metals & Materials Society), 2009

MICROSTRUCTURAL EVOLUTION DURING FRICTION STIR WELDING OF NEAR-ALPHA TITANIUM

R. W. Fonda and K. E. Knipling

Naval Research Laboratory
Code 6356, 4555 Overlook Ave., SW, Washington, DC 20375, USA

Keywords: titanium, grain structure, texture

Abstract

The microstructural evolution occurring around the tool was investigated in friction stir welds of the near-α alloy, Ti-5111. Specifically, the purpose of this investigation was to determine how the material ahead of the tool was influenced by the rotating tool to produce the refined grain structure observed adjacent to the tool and in the tool wake. This involved characterizing the base plate microstructure to show the original β grain structure and its decomposition to form specific combinations of α lath orientations. The microstructure and texture of the final refined grain structure near the tool and in the deposited weld is also discussed.

Introduction

Friction stir welding (FSW) is a solid-state joining process that was developed in the early 1990s by TWI [1]. This technique, which uses a rotating, non-consumable tool to weld the workpieces together by "stirring" together the surrounding material, was initially developed for use on aluminum alloys because of the lower temperatures and stresses required to weld those alloys and the ready availability of tool materials to perform the welding. Most of the subsequent development and commercial applications of FSW have similarly been focused on aluminum alloys. However, there is also substantial interest in developing FSW for higher strength alloys such as titanium and steels. Such applications require tools that can retain their strength at much higher temperatures and may also require welding machines that can withstand the higher loads needed for some of these alloys. Although FSW of these high strength alloys has seen much less development than FSW of aluminum alloys, FSW of many high strength alloys in titanium and steel has been demonstrated and research on the welding of these alloys is increasing [e.g., 2–14].

There has been little analysis of the microstructures and textures that are produced during FSW of titanium and steel alloys, and even less on the evolution of those microstructures and textures. This is partly due to the predominant focus of this technique on aluminum alloys, but is also due in part to the complexity that is introduced into these analyses by the allotropic phase transformations that often occurs during welding. Most titanium and steel alloys have a different crystal structure at high temperature from what is present at room temperature, and friction stir welding often induces this phase transition to occur. This can lead to complex microstructural and crystallographic changes as the weld is cooled down from the welding temperature that can be difficult to deconvolve from the evolution that occurs during the welding process.

In this study, we intend to extend some of the more recent research on the evolution and development of grain structure and crystallographic texture in aluminum alloys [15–21] to the

Report Documentation Page

Form Approved
OMB No. 0704-0188

Public reporting burden for the collection of information is estimated to average 1 hour per response, including the time for reviewing instructions, searching existing data sources, gathering and maintaining the data needed, and completing and reviewing the collection of information. Send comments regarding this burden estimate or any other aspect of this collection of information, including suggestions for reducing this burden, to Washington Headquarters Services, Directorate for Information Operations and Reports, 1215 Jefferson Davis Highway, Suite 1204, Arlington VA 22202-4302. Respondents should be aware that notwithstanding any other provision of law, no person shall be subject to a penalty for failing to comply with a collection of information if it does not display a currently valid OMB control number.

1. REPORT DATE	2. REPORT TYPE	3. DATES COVERED
FEB 2009		**00-00-2009 to 00-00-2009**

4. TITLE AND SUBTITLE	5a. CONTRACT NUMBER
Microstructural Evolution During Friction Stir Welding of Near-Alpha Titanium	5b. GRANT NUMBER
	5c. PROGRAM ELEMENT NUMBER
6. AUTHOR(S)	5d. PROJECT NUMBER
	5e. TASK NUMBER
	5f. WORK UNIT NUMBER
7. PERFORMING ORGANIZATION NAME(S) AND ADDRESS(ES) **Naval Research Laboratory,Code 6356,4555 Overlook Ave., SW,Washington,DC,20375**	8. PERFORMING ORGANIZATION REPORT NUMBER
9. SPONSORING/MONITORING AGENCY NAME(S) AND ADDRESS(ES)	10. SPONSOR/MONITOR'S ACRONYM(S)
	11. SPONSOR/MONITOR'S REPORT NUMBER(S)

12. DISTRIBUTION/AVAILABILITY STATEMENT
Approved for public release; distribution unlimited

13. SUPPLEMENTARY NOTES
See also ADM002300. Presented at the Minerals, Metals and Materials Annual Meeting and Exhibition (138th)(TMS 2009) Held in San Francisco, California on February 15-19, 2009. Sponsored in part by the Navy.

14. ABSTRACT
The microstructural evolution occurring around the tool was investigated in friction stir welds of the near-a alloy, Ti-5111. Specifically, the purpose of this investigation was to determine how the material ahead of the tool was influenced by the rotating tool to produce the refined grain structure observed adjacent to the tool and in the tool wake. This involved characterizing the base plate microstructure to show the original b grain structure and its decomposition to form specific combinations of a lath orientations. The microstructure and texture of the final refined grain structure near the tool and in the deposited weld is also discussed.

15. SUBJECT TERMS

16. SECURITY CLASSIFICATION OF:			17. LIMITATION OF ABSTRACT	18. NUMBER OF PAGES	19a. NAME OF RESPONSIBLE PERSON
a. REPORT **unclassified**	b. ABSTRACT **unclassified**	c. THIS PAGE **unclassified**	**Same as Report (SAR)**	**9**	

understanding of the comparable processes within the near-α titanium alloy, Ti 5111. This alloy was developed to exhibit a high toughness, good weldability, and good stress-corrosion cracking resistance, and is primarily considered for marine applications that require a superior toughness and corrosion resistance [22].

Experimental

The weld examined in this study is a bead-on-plate (no seam) weld in ½" (12.7 mm) thick 5111 titanium. The Ti plate was prepared at Timet, provided by Concurrent Technologies Corporation and then welded at the Edison Welding institute with a tungsten-based alloy tool at a welding speed of 2 inches per minute (0.85 mm/s) and 140 rpm, corresponding to a 360 μm tool advance per revolution. The tool used in this welding had a truncated conical geometry with a narrow shoulder and contained no threads, flats, or other features. The small size of the shoulder was selected to facilitate an even distribution of heating during the welding process because of the poor thermal conductivity of titanium.

The weld prepared using a stop-action technique wherein the tool was extracted from the plate immediately upon completion of the weld and the weld end was quenched with cold water. This process was intended to preserve the microstructure surrounding the welding tool as a representation of the actual microstructure present around the tool during the welding process. A plan-view cross section through the plate mid-thickness at the weld end, see Figure 1, was prepared by standard metallographic techniques, with final polishing accomplished using a solution of 20% hydrogen peroxide (30%) and 80% colloidal silica solution. The resultant surface was analyzed in an FEI Nova 200 NanoLab dual column field-emission gun scanning electron microscope and focused ion beam (FEGSEM/FIB) operating at 18 kV and equipped with the HKL Channel 5 system.

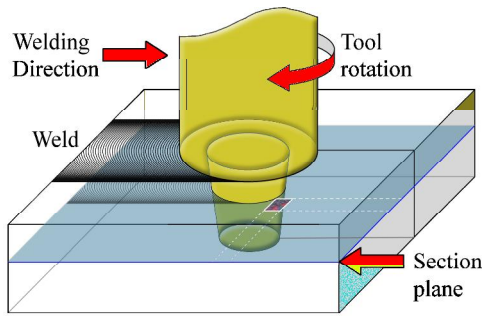

Figure 1. Schematic of the friction stir welding process showing the plan view sectioning plane used in this study and the location of Figure 2 on that sectioning plane.

Results and Discussion

Base Plate Microstructure

In order to study the microstructural evolution that occurs during friction stir welding, it is essential to understand the initial microstructure of the base plate. All microstructural evolution derives from this initial microstructure and needs to be interpreted relative to that starting point.

The microstructure of the Ti-5111 alloy consists of very large prior-β grains that can reach 8 mm in diameter (see Figure 2). These prior-β grains are subdivided into regions that contain different

α lath orientations. Some of these regions are indicated by white rectangles in Figure 2. Careful examination of these regions reveals that they each contain three specific orientations of α laths that are characterized by a 60° separation between basal $\{0001\}_\alpha$ planes and a coincidence of the close-packed $\langle 1\ 1\ -2\ 0\rangle_\alpha$ directions. Furthermore, a particular α lath orientation is only observed in one of these regions in each prior-β grain.

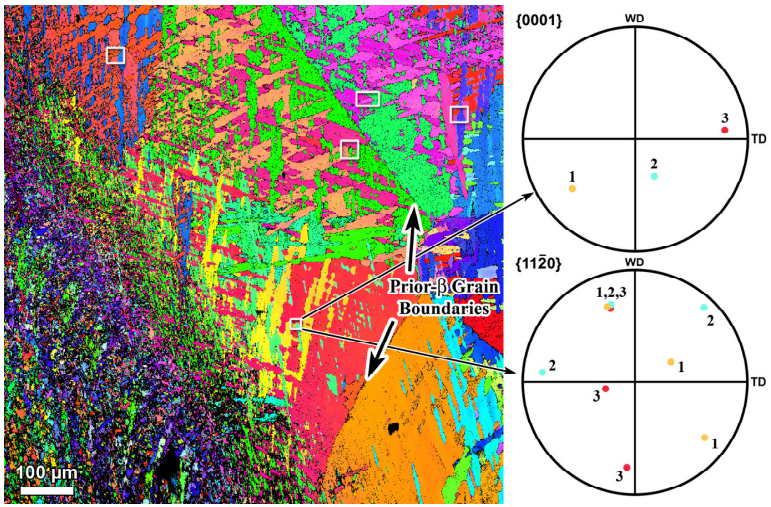

Figure 2. Plan view EBSD map of the initial grain structure ahead of the FSW tool and equal angle pole figures from the indicated region. Tool exit hole is towards the lower left, and tool rotation is clockwise.

The α laths within each prior-β grain are each related to the original β grain orientation by the Burgers orientation relationship (OR) [23], where close-packed planes $\{1\ 1\ 0\}_\beta \parallel (0\ 0\ 0\ 1)_\alpha$ and close-packed directions $\langle 1\ 1\ 1\rangle_\beta \parallel \langle 1\ 1\ -2\ 0\rangle_\alpha$ are parallel. This is the OR most commonly observed between the α and β phases in titanium [24]. From a geometric standpoint, the Burgers OR is theoretically able to generate 12 different α variants from one parent β orientation. The three α variants observed in each region of Figure 2 are the ones that share a common $\langle 1\ 1\ -2\ 0\rangle_\alpha$ direction, indicating that these are strain accommodation variants that relieve the transformation strain that each variant generates perpendicular to their common $\langle 1\ 1\ -2\ 0\rangle_\alpha$ direction.

Initial Effects of Friction Stir Welding on the Microstructure

The microstructure evolves as it approaches the rotating tool and is exposed to the increasing thermal and deformation gradients generated by the tool. The microstructural evolution occurs across a narrow (~400 μm) transition region between the unaffected base plate and the fine, equiaxed α grains near the tool, as shown in Figure 3. The initial stages of this evolution appear as a gradual refinement of the α lath structure. During this lath refinement, new crystallographic variants of α are also introduced with different lath orientations than the original variants.

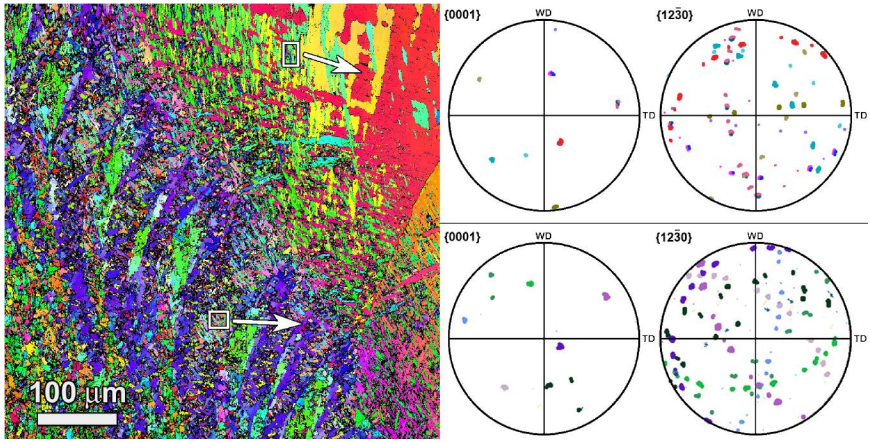

Figure 3. Plan view EBSD map of the microstructural evolution occurring through the transition region between the base plate (upper right) and the refined grain structure near the tool (lower left) and pole figures in equal angle projection showing the production of additional α variants through this transition region.

The pole figures in Figure 3 illustrate the crystallographic evolution that occurs along with this grain refinement. At the outer edge of the deformation, three additional primary orientations appear in the $\{0001\}_\alpha$ pole figure, and some minor orientations also begin to appear (see Figure 3, top pole figures). A gradual counter-clockwise rotation is apparent along with the α lath refinement as this material becomes influenced by the deformation field induced by the rotating tool. There is a discontinuity in the rotation at the outer edge of the banded region where the laths abruptly rotate approximately 10° and then retain the same orientation across the banded region (Figure 3, bottom pole figures). The same six crystallographic variants remain dominant throughout these grain rotation and refinement processes, with some additional variants appearing in minor amounts.

Other regions of the weld exhibit a more complete development of α variants that better illustrate the genesis of the observed α lath orientations. Pole figures from a region of highly refined α laths further towards the retreating side of the weld exit hole are shown in Figure 4. The symmetry of these pole figures illustrates a symmetry between the different α lath variants that demonstrates that these α lath orientations are all derived from the original β grain orientation. The six primary {0001} orientations are distributed with the angular separations of {110} poles in a bcc structure, indicating an adherence to the Burgers OR. A similar distribution of orientations can be discerned in Figure 3, although it is complicated by a greater orientation spread and the appearance of some additional variants. The Burgers OR also maintains a parallelism between the $\langle 1\ 1\ -2\ 0\rangle_\alpha$ direction and the $\langle 1\ 1\ 1\rangle_\beta$ direction, which is reflected in the three-fold symmetry evident in the $\{1\ 2\ -3\ 0\}_\alpha$ pole figure of Figure 4, but also present in Figure 3. The four-fold symmetry of the corresponding $\langle 1\ 0\ 0\rangle_\beta$ directions is evident in the $\{1\ 0\ -1\ 2\}_\alpha$ pole figure. Analysis of these pole figures reveals the presence of 12 predominant α variants. There are 6 orientation variants corresponding to an alignment of a $(0\ 0\ 0\ 1)_\alpha$ plane with one of the 6 bcc $\{1\ 1\ 0\}_\beta$ planes. Each of those plane-matching variants contains two rotational variants separated by about 10.5° to align a $\langle 1\ 1\ -2\ 0\rangle_\alpha$ close-packed direction with one of the two $\langle 1\ 1\ 1\rangle_\beta$ orientations in that $\{1\ 1\ 0\}_\beta$ plane. Thus most of the new α lath variant generation, and likely

most of the intervariant transformation, appears to arise from a local transformation to the parent β grain structure that is enabled by the high temperatures, possibly aided by the strain, of the FSW process. The subsequent decomposition of that bcc parent structure produces α laths according to the Burgers OR. Since these transformations occur through a single β grain orientation that is the same as the orientation of the original β parent grain, it is likely that small remnants of retained β were preserved between the α laths that can serve as nuclei for the allotropic α to β transformation during welding. Otherwise, multiple β grains, each of which satisfies the Burgers OR with the α laths, would be likely to form.

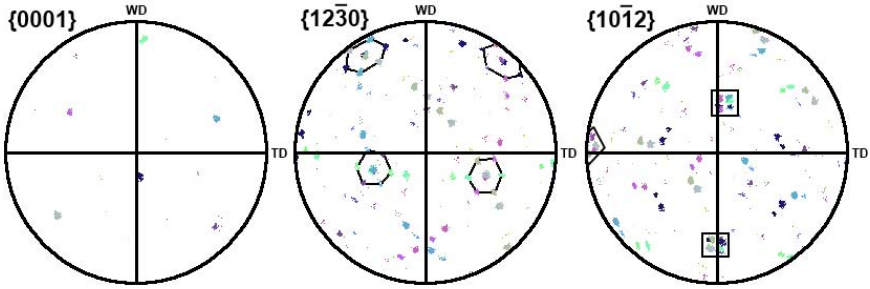

Figure 4. Pole figures in equal angle projection illustrating the cubic symmetry exhibited by the hcp α crystal variants after refinement of the lath structure and production of new α lath variants.

Texture of refined α laths in the stir zone

The predominant deformation during FSW, particularly in regions close to the tool, is expected to be simple shear, as confirmed in previous FSW studies of aluminum alloys [16, 18, 20, 21, 25, 26]. Analysis of the deformation texture that occurs around the tool during friction stir welding of this near-α titanium alloy, however, is complicated by the allotropic phase transformation. The temperatures achieved during friction stir welding of titanium alloys often exceed the transus temperature, transforming the material around the tool to the high-temperature β phase. Subsequent cooling after passage of the welding tool transforms virtually all of this material back to α, preventing a direct observation of the microstructures and textures that existed around the tool during welding. Instead, it is necessary to use the characteristics of the resultant α phase to infer the microstructure and texture that existed around the tool during welding indirectly.

The texture of this Ti-5111 friction stir weld was determined at a number of locations around the tool. Two specific locations — on the retreating side of the weld and in the deposited weld nugget — are shown in Figure 5 and typify the results obtained from all the regions examined. The left-hand pole figures, Figure 5(a), have the same relative orientation with respect to the specimen (i.e., plan view with the welding direction upward). There is a strong texture in both sets of pole figures. The basal $\{0\ 0\ 0\ 1\}_\alpha$ planes are tilted ~35° from ND in the direction away from the welding tool and the $\langle 1\ 1\ -2\ 0\rangle_\alpha$ directions are aligned tangent to the tool, which is parallel to the presumed direction of maximum shear.

The pole figures can be rotated into the shear deformation frame of reference, with a horizontal shear direction (SD) and a vertical shear plane normal (SPN), as shown in Figure 5(b). The geometry of the tool can be used to determine the orientation of the SD and SPN adjacent to the tool at those locations. The SD can be assumed from the tool tangent. Aligning the pole figures with this presumed shear direction aligns the predominant $\langle 1\ 1\ -2\ 0\rangle_\alpha$ direction with the

horizontal axis of the pole figure. The shear plane is parallel to the surface of the truncated conical tool, which has a taper angle of ~27° (see tool schematic in Figure 5). Rotating the pole figure to account for this taper aligns a $\{0\ 0\ 0\ 1\}_\alpha$ orientation near the ND. Thus, the close-packed $\{0\ 0\ 0\ 1\}_\alpha$ basal plane appears to be perpendicular to the shear plane and the close-packed $<1\ 1\ -2\ 0>_\alpha$ directions are parallel to the SD. The pole figures shown in Figure 5(b) reflect this local orientation of the texture.

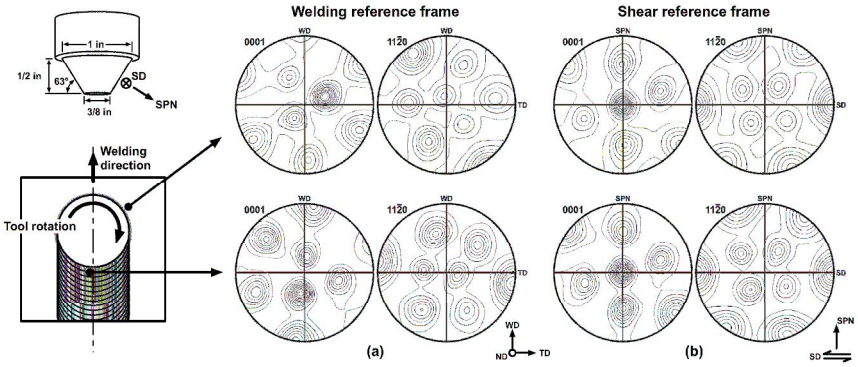

Figure 5. Schematics of the FSW tool geometry and the end of the weld, indicating the locations adjacent to the exit hole from which the $\{0\ 0\ 0\ 1\}_\alpha$ and $\{1\ 1\ -2\ 0\}_\alpha$ pole figures shown in parts (a) and (b) (in stereographic projection) were obtained. In (a), the pole figures have the same orientation as in the weld schematic. In (b), the pole figures have been rotated to align the presumed shear plane normal (SPN) with the vertical direction and the shear direction (SD) with the horizontal direction. The contours shown in the pole figures are multiples of 0.5 times random density.

In bcc metals, simple shear deformation produces partial fibers belonging to $\{hkl\}\langle 111\rangle$ and $\{110\}\langle uvw\rangle$, as established by modeling and experimental studies of deformation textures in torsion tests [e.g., 27–28]. The texture components of these ideal simple shear orientations are shown in the $\{110\}_{bcc}$ pole figure, Figure 6(a). Figure 6(b) displays these $\{110\}_{bcc}$ ideal shear orientations from Figure 6(a) superimposed on the $\{0001\}_\alpha$ pole figure from the deposited weld (bottom of Figure 5(b)). This Figure reveals an extremely good agreement between the experimental $\{0001\}_\alpha$ texture and the ideal $\{110\}_{bcc}$ shear texture, which is expected since these close-packed planes are parallel according the Burgers OR. Figure 6 demonstrates that the observed $\{0001\}_\alpha$ texture is inherited directly from the shear texture of the high-temperature β phase, and closely matches the $D\{112\}\langle 111\rangle$ texture component.

There have been two previous FSW studies on the texture produced in titanium alloys that should be compared to these results. Reynolds et al. [8] studied friction stir welds of a β titanium alloy and observed excellent agreement between the observed shear texture in the weld nugget (after a rotation of the pole figures) and the shear textures of bcc tantalum reported by Rollet and Wright [29]. Mironov et al. [30] measured the stir zone texture developed in friction stir welds of an α-β titanium alloy, Ti-6Al-4V, and found that the retained β phase exhibited a $\bar{J}\{\bar{1}\,\bar{1}\,0\}\langle\bar{1}\,1\bar{2}\rangle$ simple shear texture that presumably developed from $\{110\}\langle 111\rangle$ slip. The authors, however, admitted that the small amount of retained β in that sample limited the statistics supporting this result.

Mironov et al. [31] also measured the texture developed from friction stir processing of pure iron and consistently observed, from several locations within the stir zone, a $D_2(11\bar{2})[111]$ simple shear texture. Moreover, this $D_2(11\bar{2})[111]$ texture is the one most commonly observed during equal channel angular extrusion of bcc iron [32,33]. The similar texture produced during the current examination of friction stir welding of Ti-5111, friction stir processing of pure iron, and the equal channel angular extrusion of bcc iron further supports the conclusion that the texture observed near the FSW tool and in the deposited weld is directly derived from a simple shear texture of the high-temperature β phase.

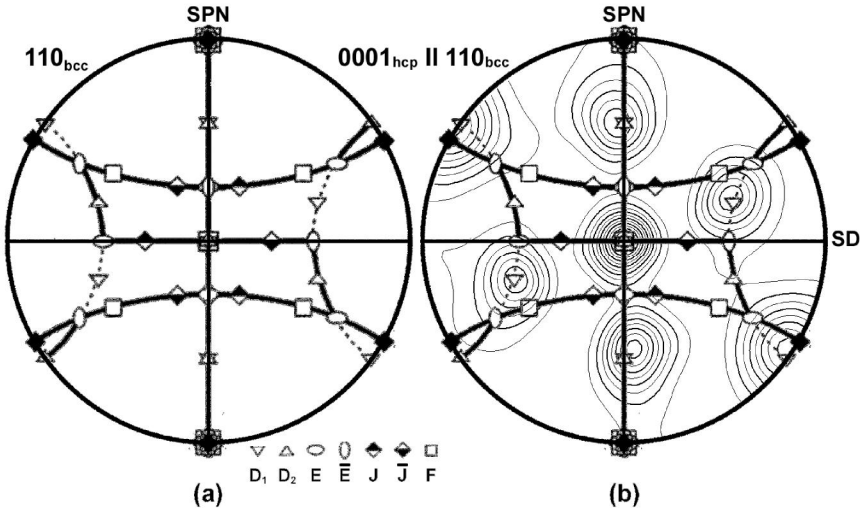

Figure 6. (a) Schematic {110} pole figure in stereographic projection showing the main simple texture component orientations and fibers associated with simple shear deformation of bcc metals (after Li et al. [31]). (b) Superposition of the simple shear texture components on the {0001} pole figure of the deposited weld (rotated into the shear reference frame) from Figure 5(b).

Conclusion

The microstructural evolution occurring during friction stir welding of a near-α titanium alloy, Ti-5111, was discussed. The microstructure transitions over ~400 μm from the unaffected base plate, which consists of course α laths within prior-β grains, to a fine equiaxed α microstructure near the tool. In the unaffected baseplate, the α laths are related to the original β grain orientation by the Burgers OR, which aligns close-packed planes $\{1\ 1\ 0\}_\beta \parallel (0\ 0\ 0\ 1)_\alpha$ and close-packed directions $\langle 1\ 1\ 1\rangle_\beta \parallel \langle 1\ 1\ -2\ 0\rangle_\alpha$. Prior-β grains are typically subdivided into regions that each contain three α variants that share a common $\langle 1\ 1\ -2\ 0\rangle_\alpha$ direction, indicating that these are strain accommodation α variants. Closer to the tool, there is as a gradual refinement of the α laths, which also rotate slightly in response to the shear deformation generated by the tool. Additional α variants are also generated through this region that are derived from the original β grain orientation. Adjacent to the FSW tool, the high temperatures and extensive shear deformation results in refined grains of α exhibiting a $\{0001\}_\alpha$ basal texture closely matching the

$D_2(11\bar{2})[111]$ simple shear texture observed in high-temperature torsion and equal channel angular extrusion (ECAE) of bcc iron. This indicates that the observed α texture in the stir zone is inherited directly from a simple shear texture of the high-temperature β phase.

References

1. W.M. Thomas, E.D. Nicholas, J.C. Needham, M.G. Murch, P. Templesmith, and C.J. Dawes, "Friction Stir Butt Welding", Int. Patent App. PCT/GB92/02203 and GB Patent App. 9125978.8, Dec. 1991. U.S. Patent No. 5,460,317, Oct. 1995.
2. W.M. Thomas, P.L. Threadgill, E.D. Nicholas, "Feasibility of Friction Stir Welding Steel", *Sci Tech Weld Join*, **4**, 365-372 (1999).
3. A.P. Reynolds, W. Tang, M. Posada, and J. DeLoach, "Friction Stir Welding of DH36 Steel", *Sci Tech Weld Join*, **8**, 455-460 (2003).
4. P.J. Konkol, J.A. Mathers, R. Johnson, and J.R. Pickens, "Friction Stir Welding of HSLA-65 Steel for Shipbuilding", *J Ship Production*, **19**, 159-164 (2003).
5. M. Posada, J. DeLoach, A. P. Reynolds, R. W. Fonda, and J. P. Halpin, "Evaluation of Friction Stir Welded HSLA-65", *Proc 4th Int Symp on FSW*, TWI Ltd., S10A-P3 (2003).
6. A.J. Ramirez and M.C. Juhas, "Microstructural Evolution in Ti-6Al-4V Friction Stir Welds", *Mat Sci Forum*, **426-4**, 2999-3004 (2003).
7. T.W. Nelson, J.-Q. Su, and R.J. Steel, "Friction Stir Welding of Ferritic Steels", *Proc 14th Int Offshore and Polar Eng Conf*, 50-54 (2004).
8. A.P. Reynolds, E. Hood, and W. Tang, "Texture in Friction Stir Welds of Timetal 21S", *Scripta Mater*, **52**, 491-494 (2005).
9. Y.S. Sato, T.W. Nelson, and C.J. Sterling, "Recrystallization in Type 304L Stainless Steel During Friction Stirring", *Acta Mater*, **53**, 637-645 (2005).
10. W.B. Lee, C.Y. Lee, W.S. Chang, Y.M. Yeon, S.B. Jung, "Microstructural Investigation of Friction Stir Welded Pure Titanium", *Mat Sci Lett*, **59**, 3315-3318 (2005).
11. S.H.C. Park, Y.S. Sato, H. Kokawa, K. Okamoto, S. Hirano, M. Inagaki, "Microstructural Characterisation of Stir Zone Containing Residual Ferrite in Friction Stir Welded 304 Austenitic Stainless Steel ", *Sci. Technol. Weld. Joining*, **10**, 550–56 (2005)
12. A.L. Pilchak, M.C. Juhas, and J.C. Williams, "Microstructural Changes due to Friction Stir Processing of Investment-cast Ti-6Al-4V", *Met Mat Trans A*, **38A**, 401-408 (2007).
13. S. Mironov, Y. Zhang, Y.S. Sato, and H. Kokawa, "Development of Grain Structure in β-Phase Field During Friction Stir Welding of Ti-6Al-4V Alloy", *Scripta Mater*, **59**, 27-30 (2008).
14. S. Mironov, Y. Zhang, Y.S. Sato, and H. Kokawa, "Crystallography of Transformed β Microstructure in Friction Stir Welded Ti-6Al-4V Alloy", *Scripta Mater*, **59**, 511-514 (2008).
15. J.-Q. Su, T.W. Nelson, R. Mishra, and M. Mahoney, "Microstructural Investigation of Friction Stir Welded 7050-T651 Aluminium", *Acta Mater*, **51**, 713-729 (2003).
16. R.W. Fonda, J.F. Bingert, and K.J. Colligan, "Development of Grain Structure During Friction Stir Welding", *Scripta Mat*, **51**, 243-248 (2004).
17. J.A. Schneider and A.C. Nunes, Jr, "Characterization of Plastic Flow and Resulting Microtextures in a Friction Stir Weld", *Met Mat Trans B*, **35B**, 777-783 (2004).
18. P.B. Prangnell and C.P. Heason, "Grain Structure Formation During Friction Stir Welding Observed by the 'Stop Action Technique'", *Acta Mater*, **53**, 3179-3192 (2005).
19. R.W. Fonda and J.F. Bingert, "Precipitation and Grain Refinement in a 2195 Al Friction Stir Weld", *Met Mat Trans A*, **37A**, 3593-3604 (2006).

20. R.W. Fonda, J.A. Wert, A.P. Reynolds, and W.Tang, "Friction Stir Welding of Single Crystal Aluminum", *Sci Tech Weld Join*, **12**, 304-310 (2007).
21. R. W. Fonda, K. E. Knipling, and J. F. Bingert, "Microstructural Evolution Ahead of the Tool in Aluminum Friction Stir Welds", *Scripta Mater*, **58**, 343-348 (2007).
22. Titanium Metal Corporation: TIMETAL 5111, Report # TMC-0170, Titanium Metal Corporation, Denver, Co, (2000).
23. W. G. Burgers, "On the Process of Transition of the cubic-body-centered Modification into the hexagonal-close-packed Modification of Zirconium," *Physica*, **1**, 561–586 (1934).
24. G. Lutjering and J. C. Williams, Titanium, Springer-Verlag, pp. 27–31 (2003).
25. Y.S. Sato, H. Kokawa, K Ikeda, M. Enomoto, S. Jogan, and T. Hashimoto, "Microtexture in the Friction-Stir Weld of an Aluminum Alloy", *Met Mat Trans A*, **32A**, 941-948 (2001).
26. D.P. Field, T.W. Nelson, Y. Hovanski, and K.V. Jata, "Heterogeneity of Crystallographic Texture in Friction Stir Welds of Aluminum", *Met Mat Trans A*, **32A**, 2869-2877 (2001).
27. F. Montheillet, M. Cohen, and J. J. Jonas, "Axial Stresses and Texture Development During the Torsion Testing of Al, Cu and α-Fe," *Acta Metall*, **32**, 2077–2089 (1984).
28. J. Baczynski and J. Jonas, "Texture development during the torsion testing of alpha-iron and two IF steels," *Acta Mater*, 44, 4273–4288 (1996).
29. A. D. Rollett and S. I. Wright, in Texture and Anisotropy, edited by U. F. Kocks, S. N. Tome, and H. R. Wenk (Cambridge University Press, 1998), p. 202.
30. S. Mironov, et al., "Development of Grain Structure in β-Phase Field during Friction Stir Welding of Ti-6Al-4V Alloy," *Scripta Mater*, **59**, 27–30 (2008).
31. S. Mironov, Y. S. Sato, and H. Kokawa, "Microstructural Evolution during Friction Stir-Processing of Pure Iron," *Acta Mater*, **56**, 2602–2614 (2008).
32. S. Li, I. J. Beyerlein, and M. A. M. Bourke, "Texture Formation during Equal Channel Angular Extrusion of fcc and bcc Materials: Comparison with Simple Shear," *Mater Sci Eng A*, **394**, 66–77 (2005).
33. A. A. Gazder, et al., "Microstructure and Texture Evolution of bcc and fcc Metals Subjected to Equal Channel Angular Extrusion," *Mater Sci Eng A*, **415**, 126–139 (2006).